Torres-Herrador, F.; Leroy, V.; Helber, B.; Contat-Rodrigo, L.; Lachaud, J.; Magin, T. (2020). Multicomponent Pyrolysis Model for Thermogravimetric Analysis of Phenolic Ablators and Lignocellulosic Biomass. AIAA Journal. 58(9):4081-4089. https://doi.org/10.2514/1.J059423

Multicomponent Pyrolysis Model for Thermogravimetric Analysis of Phenolic Ablators and Lignocellulosic Biomass

F. Torres-Herrador,* V. Leroy,† and B. Helber‡
von Karman Institute for Fluid Dynamics, 1640 Rhode-Saint-Genèse, Belgium
L. Contat-Rodrigo§
Polytechnic University of Valencia, 46022 Valencia, Spain
J. Lachaud¶
University of Bordeaux, 33405 Talence, France
and
T. Magin**
von Karman Institute for Fluid Dynamics, 1640 Rhode-Saint-Genèse, Belgium

https://doi.org/10.2514/1.J059423

A multicomponent kinetic mechanism has been developed for the pyrolysis at low heating rate of carbon/phenolic thermal protection material and a wood species. An experimental campaign has been carried out using thermogravimetric analysis to study the mass loss under different conditions of crucible (with or without a lid) and heating rate for both materials. Using a pierced lid to cover the crucible during pyrolysis promotes char production compared with the case of open crucible. Kinetic parameters were then extracted from the experiments by an optimization approach using an in-house-developed kinetic identification code. The parameters recovered for the two applications allow to reproduce accurately the mass loss evolution.

Nomenclature

$\mathcal{A}$	=	preexponential factor
$\mathcal{E}$	=	activation energy, kJ · mol^{-1}
m	=	mass, kg
n	=	order of the reaction
$\mathcal{R}$	=	universal gas constant, J · K^{-1} · mol^{-1}
β	=	heating rate, K/min
χ	=	advancement of the reaction
ρ	=	density, kg · m^{-3}

Subscripts

amb	=	ambient conditions
c	=	charred material
v	=	virgin material
0	=	initial conditions
∞	=	final conditions

I. Introduction

AFTER the success of the Stardust mission in 2006, the use of lightweight carbon/phenolic composites as ablative thermal protection system (TPS) for spacecraft has grown [1–5]. Ablative heat shields are the sole solution when considering sample return from Mars or asteroids due to the high reentry speeds, which result in high heat fluxes on the spacecraft surface [6,7]. In ablative TPS, these high fluxes are partly dissipated by physical and chemical decomposition. One of the most important chemical processes is the pyrolysis of the phenolic resin [8]. The resin is thermally decomposed in several stages absorbing energy (endothermic reactions), thus protecting the spacecraft. In addition, pyrolysis gases are blown in the boundary layer providing extra protection against the high-enthalpy plasma [9]. However, pyrolysis mechanisms by which the resin is decomposed are not yet fully understood. Accurate description of this process would allow for a reduction in the safety factors currently in use for TPS design [10].

Pyrolysis is encountered in many other applications; for example, it is one of the chemical processes that occur when biomass is submitted to high-temperature conditions. When biomass waste (e.g., scrap lumber, forest debris, crops) gets thermally degraded, it releases gases, which are classified into organic volatile compounds, tars (if they condense at room temperature), and charcoal [11]. This process is of special interest for industrial applications because the obtained products can be used as renewable fuels or fertilizers. The prediction of the generation of each product is an important challenge due to the variability of wood species and the complex chemical reactions involved [12].

Modern studies on biomass pyrolysis started in the 1960s with the work of Broido and Kilzer [13], and nowadays a large database is available (~13,044 results in Scopus for 1978–2019, keywords: `biomass pyrolysis`). Similarly, modern studies on phenolic pyrolysis for the TPS application started in the 1960s [14] but, in contrast, the community has devoted fewer resources afterward, in particular because space exploration has been less preeminent after the Apollo program (~67 results for the same period of time, keywords: `phenolic ablator pyrolysis`). In the literature of biomass, one encounters different pyrolysis models (multicomponent, competitive, isoconversional, distributed activation energy, etc.), whereas aerospace has been limited to multicomponent mechanisms [15,16], until a phenomenological competitive mechanism was developed [17] recently. In addition, the biomass community has large experience on diagnostics for identification and quantification of pyrolysis products coupling advanced techniques such as mass spectrometry and gas chromatography [18]. These techniques have been used in aerospace also in recent works [19,20] separately.

In an effort to bridge the gap between biomass and aerospace developments, we analyze in this work one class of carbon/phenolic TPS material (ZURAM) and one endemic wood species from the Pacific islands (niaouli). With these two examples, we will demonstrate that the degradation process (i.e., pyrolysis) is similar when these materials are exposed to high temperature, and many developments

Received 14 January 2020; revision received 12 April 2020; accepted for publication 3 May 2020; published online 27 May 2020.

*Ph.D. Candidate, Aeronautics and Aerospace Department.
†Postdoctoral Researcher, Aeronautics and Aerospace Department.
‡Research Engineer, Aeronautics and Aerospace Department.
§Professor, Department of Thermal Engines and Machines.
¶Assistant Professor, Institute of Mechanics and Engineering.
**Professor, Aeronautics and Aerospace Department.

Table 1 Microstructural analogy between ablative TPS and biomass

Component	Ablative TPS (ZURAM)	Biomass (niaouli)
Fiber	Carbon fibers	Cellulose
Resin	Phenolic resin	Lignin, hemicellulose

can be transferred from one application to the other. In fact, wood species such as cork are commonly used as base material for the development of TPS. For example, resin-reinforced cork (P50) has been used in several atmospheric entry applications [21,22].

Similarity of the material thermal properties comes from their comparable microstructure and composition. Both wood and TPS can be seen as composite materials as illustrated in Table 1. The two materials are made of fibers, which are embedded in a resin that provides structural cohesion (Fig. 1). Their high porosity will reduce the effective thermal conductivity. However, an important difference is that, in the case of ablative TPS, the carbon fibers will not pyrolyze, whereas the wood cellulose will pyrolyze at $T \approx 600$ K [23].

The objectives of this work are 1) to highlight the similarities between the two problems, 2) to develop a common methodology for the analysis of data to show how the development of carbon/phenolic ablative heat shields can benefit from the large amount of research carried out by the biomass scientific community, and 3) to characterize the thermal degradation of a lightweight carbon/phenolic material for TPS.

This paper is organized as follows. Section II presents the pyrolysis model proposed for these materials. In Sec. III, the two materials that we have analyzed are presented, as well as the thermal analyzer used to perform the measurements. The experimental results are presented in Sec. IV.A. A parameter identification tool (FiTGA) has been developed and applied to the aforementioned experiments (Sec. IV.B). Conclusions are drawn in Sec. V.

II. Pyrolysis Modeling

It is commonly accepted [11,24,25] that a global pyrolysis reaction can be represented using an Arrhenius expression:

$$\frac{\mathrm{d}\chi}{\mathrm{d}t} = \mathcal{A}(1-\chi)^n \exp\left(-\frac{\mathcal{E}}{\mathcal{R}T(t)}\right) \tag{1}$$

This function provides information on the evolution in time of a particular global reaction being the advancement of reaction $\chi = 0$, when it has not started, and reaching $\chi = 1$ at the end of the process. The parameters $\mathcal{A}$, n, and $\mathcal{E}$ are, respectively, the preexponential factor, the order of the reaction, and the activation energy. These kinetic parameters control the reaction rate, but their actual physical meaning in pyrolysis, contrary to gas reactions, is still subject to debate [26–28].

In most cases, a single reaction is not capable of reproducing the decomposition of a complex material. Therefore, combinations of the above expression are in use. Di Blasi [11] presents an extensive review on pyrolysis modeling. In this case, we focus on multicomponent (parallel) kinetic schemes, which are commonly used in aerospace.

Multicomponent kinetic schemes make the assumption that the different reactions are independent from one another. In other words, one can consider that the material is composed of solid phases, denoted by the subscript i, which sublimate into gases with given predefined proportions. This model makes use of the mass loss fraction F_i, which relates the advancement χ_i with the actual mass loss through

$$m(t) = m_0\left(1 - \sum_{i=1}^{N} F_i \chi_i(t)\right) \tag{2}$$

The reference model in TPS design [29][††] (Fig. 2), which is an evolution from the models of Goldstein [14] and Trick et al. [30], uses parallel schemes. Parallel schemes can also be found in biomass literature with the works of Shafizadeh and Chin [23] or Park et al. [24].

[††]A typo was found in the F factor of C_6H_6O in the cited reference, which has been corrected here: $F_{C_6H_6O} = 0.29$.

III. Materials and Methods

A. Ablative TPS: ZURAM®

Even though there are several publications about ablative TPS materials, data or the material itself cannot be easily shared in the scientific community because of confidentiality reasons. In an attempt of having a reference material for research purposes, the German Aerospace Center (DLR) has developed the new lightweight ablative material ZURAM [31] to be used for the validation of computational tools, being a candidate to replace the Theoretical Ablative Composite for Open Testing (TACOT) [32], which is currently used for code-to-code verification.

An important characterization effort on ablative thermal protection materials is being done at the von Karman Institute for fluid dynamics (VKI) using thermal analysis (thermogravimetric analysis [TGA]/differential scanning calorimetry) for a detailed response as well as plasma tests for a global response [33–35].

This material shares similarities with other TPS materials such as Asterm (Airbus) or Phenolic-Impregnated Carbon Ablator (PICA; NASA) [36]. However, the density of ZURAM is slightly higher ($\rho_{\mathrm{PICA}} \approx 270$ kg $\cdot$ m^{-3}, $\rho_{\mathrm{ZURAM}} \approx 380$ kg $\cdot$ m^{-3}). In addition, even though the raw materials are generically the same (carbon fibers and phenolic resin), differences in composition of the materials may be expected as well as differences in manufacturing (curing) processes, which cannot be publicly accessed. The samples of ZURAM were provided in form of plates of size $20 \times 20 \times 5$ cm^3.

B. Plant Biomass: Niaouli

In the past, several wood species have been the subject of thermal degradation studies, oak and beech being the most common ones [37,38]. As part of collaboration with the University of New Caledonia, it was decided to analyze an endemic plant, niaouli, which has been proven to have an exceptional resistance against wild fires [39]. This tree has a laminated, porous, and thick external bark, which is responsible for its fire resistance. The samples of niaouli were provided in form of wood powder, with a particle size of ~0.5 mm.

C. Sample Preparation

After some preliminary testing using carbon preform, we realized that the low density of ZURAM and the poor thermal contact sample crucible hinder accurate and repeatable measurements. Therefore, following the recommendations of [40], it was decided to crush the materials in small particles. The ZURAM material was crushed using a mortar, resulting in dust; particle size was not accurately measured. Niaouli was already provided in powder form as aforementioned. Both materials were stored in glass vials and introduced in the argon glovebox where the simultaneous thermal analyzer (STA) is located. They remained there for 3 days before the experiments started to ensure that any air or humidity introduced would get removed by diffusion. The samples were prepared by taking material from the vials at random with a microspoon, inserted in the crucible and slightly compressed manually using a Teflon rod. The crucibles were carefully cleaned using a foam swab before introducing them in the STA.

Crushing the material has two main positive effects:

1) It increases the mass of sample material in the crucible (~25 mg), thus improving sensitivity.

2) It improves contact between the sample and the crucible.

However, by crushing the test samples, the impact of microstructure on pyrolysis (if any) cannot be studied.

The temperature homogeneity after the packing was assessed by performing numerical simulations with the Porous material Analysis Toolbox based on OpenFoam (PATO) using data from the TACOT. These simulations (Fig. 3) showed that the differences between the center of the crucible and the external part were not higher than 0.15 K.

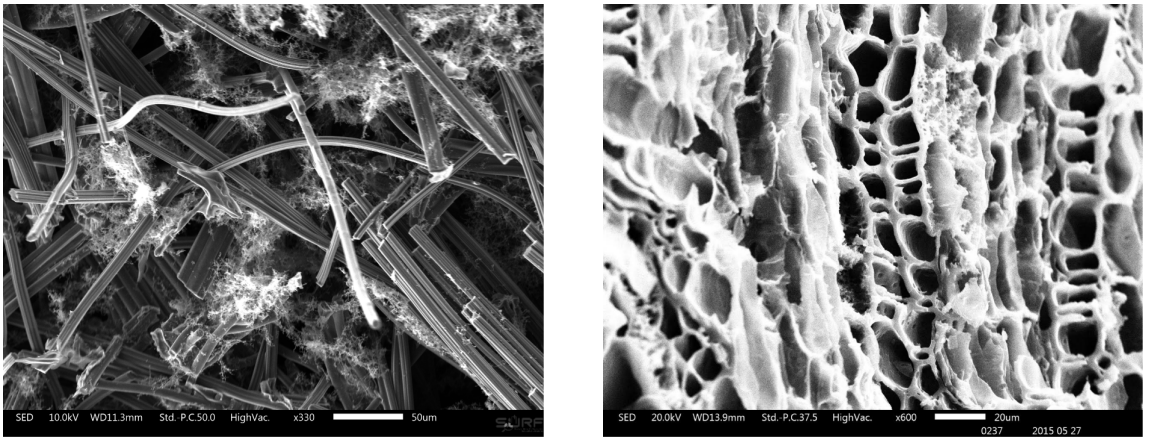

a) Partially pyrolyzed carbon/phenolic ablator ZURAM®. The carbon fibers and the phenolic resin around them are observed

b) Niaouli after pyrolysis. The empty cells are observed separated by the cell walls [29]

Fig. 1 Scanning electron microscopy images of the two materials studied.

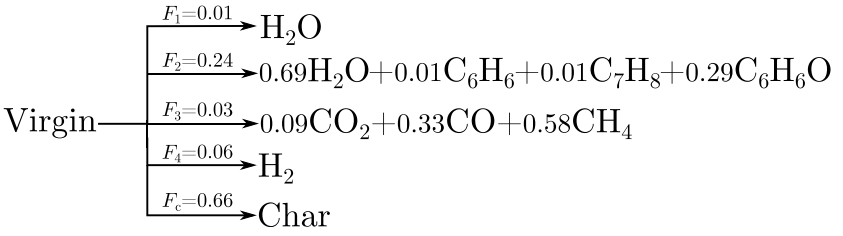

Fig. 2 Parallel kinetic scheme from Lachaud et al. [29] illustrating how the mass loss fractions F_i are fixed.

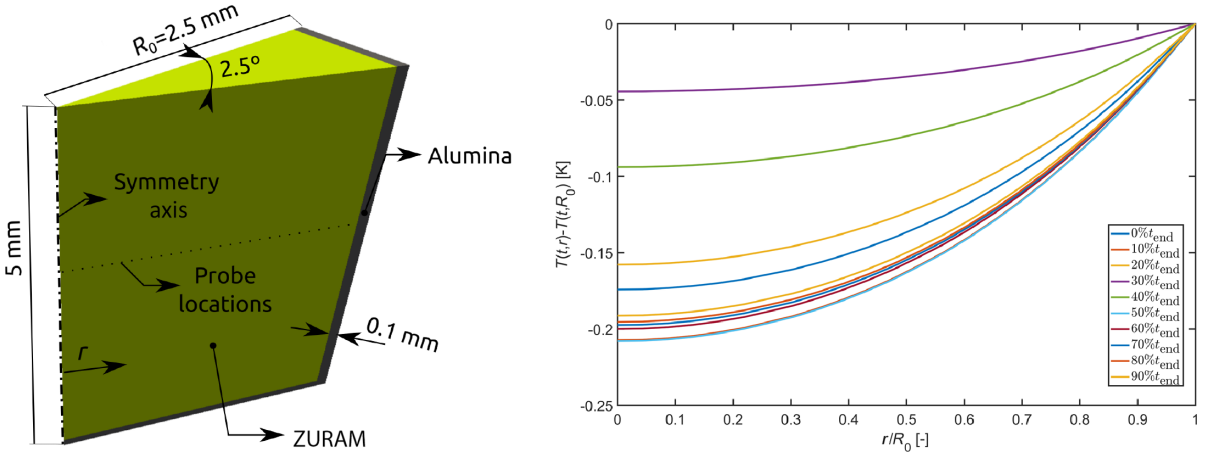

a) Crucible simulation setup

b) Temperature difference between the center of the sample and the external wall

Fig. 3 Simulation of the TGA crucible to assess temperature homogeneity using PATO.

D. Thermogravimetric Analysis

TGA is a thermal analysis technique in which the mass of a sample is monitored while following an imposed temperature program. A common practice consists of increasing the temperature at a constant heating rate (i.e., $\beta = 10\ \mathrm{K \cdot min^{-1}}$).

To identify global reactions, the TGA curve (or thermogram) and its derivate DTGA[‡‡] are usually examined. Figure 4 presents an example of a thermogram generated with dummy synthetic data. In the DTGA (solid line), one observes two peaks, which would correspond to two global reactions achieving their maximum at $T_{\mathrm{peak1}} = 600$ K and $T_{\mathrm{peak2}} = 1100$ K. Each reaction produces mass loss, achieving a final mass of 70% (dashed line).

TGA measurements were performed using the STA *449 F3 Jupiter* of NETZCH. The STA is located inside a glovebox with controlled conditions ($T_{\mathrm{amb}} = 21°\mathrm{C}$, $p_{\mathrm{amb}} = 1$ bar; purge gas: argon $100\ \mathrm{mL \cdot min^{-1}}$).

This STA allows different configurations depending on the application. In the present case, the interest was to reach high temperatures, ensuring complete pyrolysis. Therefore, it was decided to use alumina (Al_2O_3) crucibles and a platinum furnace, allowing a maximum temperature of 1700 K measured using type S thermocouples. The STA was calibrated following the standard procedure of the manufacturer based on the known melting point of six different metals.

[‡‡]For convention and clarity, DTGA curves are represented with an implicit negative sign, such that mass loss peaks are positive.

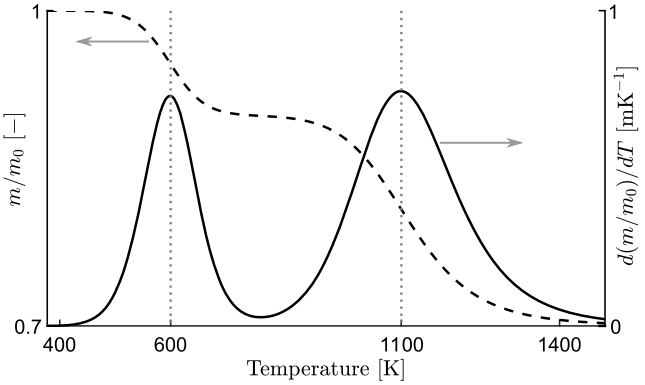

Fig. 4 Example of TGA (left) and DTGA (right) curves generated with dummy data.

We have considered two experimental conditions in our study: different heating rates ($\beta = 5$, 20, and 40 K · min^{-1}) and the use of a lid during the measurements.

Previous researchers [11,41] showed that compensation effects between the parameters are found when identifying kinetic parameters from TGA experiments. To overcome this problem, it was recommended to carry out the parameter identification using several sets of data obtained at different heating rates [42], thus constraining the problem and leading to a unique solution.

The use of a lid during TGA experiments has been debated in the biomass community for many years. Using a (possibly pierced) lid results in released gases being trapped with the sample. They provide a "self-generated" atmosphere inside the crucible, at a pressure slightly higher than the atmospheric pressure. The lid also increases the residence time for pyrolysis gases [43]. Consequently, the hot gases may eventually react and recombine, thus creating various species that may deposit on the fibers or the crucible. Without a lid, one encounters an isobaric measurement with faster evacuation of the hot pyrolysis gases [44]. In addition, it is not clear which condition is more similar to the pyrolysis of an ablator in flight conditions. A pierced lid may provide more similitude deeper inside the material, where the pyrolysis gas has a higher residence time. An open lid may provide more similitude close to the surface. Nevertheless, most literature on identification of kinetic parameters through TGA uses an open lid approach in order to avoid secondary char formation reactions.

E. Fitting TGA Algorithm

In addition to the experimental work, we have developed a tool, Fitting TGA Algorithm (FiTGA), capable of identifying kinetic parameters using optimization techniques. We have applied this identification method to the TGA data collected for ZURAM and niaouli.

FiTGA, developed in MATLAB, includes the following optimization algorithms: 1) gradient algorithm (nonlinear least-squares method [LSQ] [45]), and 2) gradient-free algorithms (shuffled complex evolutionary [SCE] [46] and genetic algorithm [GA] [47]).

FiTGA first uses a gradient-free algorithm (GA or SCE) to get a global, accurate solution with low precision. The software then switches to a gradient-based LSQ method to refine the first estimate and get a precise solution.

Figure 5 depicts the workflow of FiTGA when using a GA algorithm. Bounds for each variable have to be provided by the user. With this information, the algorithm will reconstruct the mass loss curve by integrating the parallel kinetic scheme. This reconstructed curve will be compared with the experimental data calculating L2-norm until convergence.

IV. Results and Discussion

In the following sections, both the experimental and the parameter identification results are presented for the two materials studied.

A. TGA Characterization

Hereafter, the results of our experiments are presented, particularized for the case of $\beta = 5$ K · min^{-1}. Analogous results were obtained for the other heating rates, which are presented in the Appendix.

1. *Niaouli*

Figure 6a presents the averaged results obtained for niaouli (with and without lid) at $\beta = 5$ K · min^{-1}. One can observe four peaks on

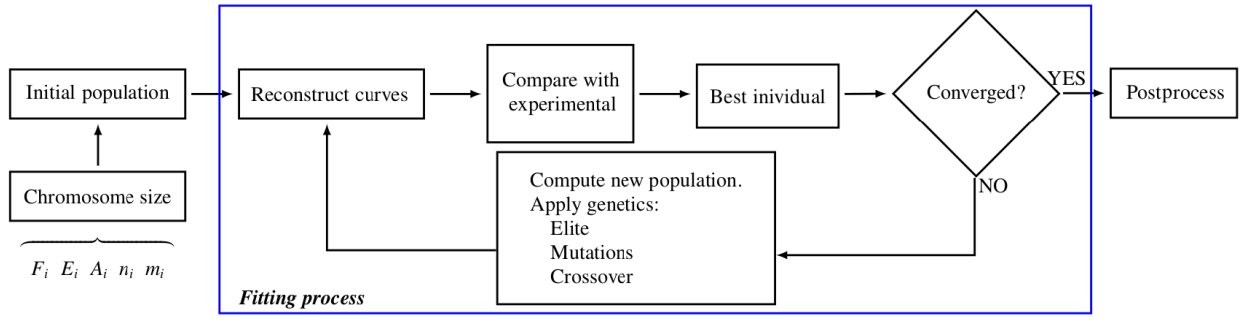

Fig. 5 Flowchart for the genetic algorithm implemented in FiTGA.

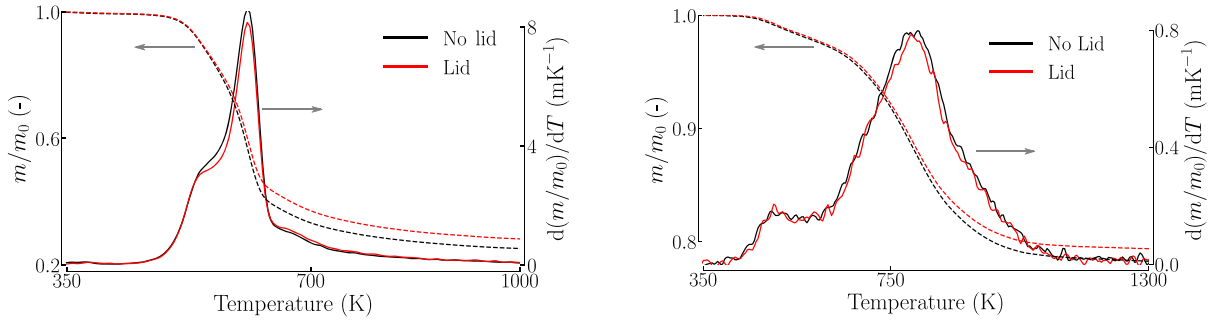

a) TGA (left) & DTGA (right) for niaouli **b) TGA (left) & DTGA (right) curves for ZURAM®**

Fig. 6 Experimental results for niaouli (left) and ZURAM (right) at $\beta = 5$ K · min^{-1} showing the decrease of mass loss when using a lid during the measurements.

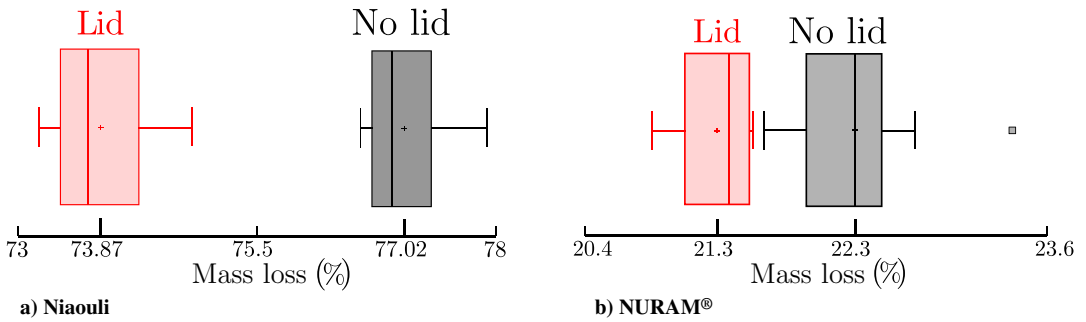

a) Niaouli b) NURAM®

Fig. 7 Box plots of niaouli (left) and ZURAM (right) containing the mass loss data from all the measurements. A significant change in mass loss is observed in the two materials.

the DTGA signal, which correspond, respectively [23], to the evaporation of water ($T^{\text{peak}}_{\text{H}_2\text{O}} \approx 380$ K) and the pyrolysis of hemicellulose ($T^{\text{peak}}_{\text{hemicell}} \approx 550$ K), cellulose ($T^{\text{peak}}_{\text{cell}} \approx 600$ K), and lignin ($T^{\text{peak}}_{\text{lignin}} \approx 650$ K), reaching a final mass of ~25%.

In addition, at $T \approx 580$ K, the two DTGA curves shown in Fig. 6a differ. This effect results in a difference on the final char yield (3%). This result is in agreement with the results of Rath et al. [43] and Roberts [48], who concluded that using a lid promotes secondary char formation reactions.

An analogous conclusion was given by Mok and Antal [49], who performed experiments on cellulose in a pressure-variable thermal analyzer. An increase of pressure promotes the formation of char through the aforementioned secondary char reactions, reaching variations of up to 20% in the final mass.

The aforementioned 3% char difference was observed in all our experiments for the different heating rates. To study whether this difference was significant, we performed statistical analysis using the Student t test. This test allows the comparison of the mean of two populations assuming equal variances. Because the samples were extracted from the same bulk material, the variance, which can be attributed to differences in composition, can be considered equal for the two types of experiments. If $p_{\text{value}} < 0.05$, the null hypothesis of equal means can be rejected, implying that there is a significant difference between the means of the two types of experiments (lid and no lid).

The p_{value} calculated at a confidence level of 95% was 2.73×10^{-10}, thus rejecting the null hypothesis of equal means. This confirms that there is a significant difference between the experiments performed with and without lid. This is also illustrated by the box plots of Fig. 7a.

From this result, we conclude that variations on the experimental conditions provide significant changes on the final mass of char.

2. *ZURAM*

Similarly to the previous section, Fig. 6b presents the results obtained for the TPS material ZURAM. The total decomposition of this material barely reaches a ~20% decomposition.[§§]

In this case, the DTGA signal presents two main peaks ($T_{\text{peak1}} \approx 500$ K and $T_{\text{peak2}} \approx 800$ K). Studies performed by Wong et al. [50,51] and by Bessire and Minton [20,52] on PICA suggest that the mass loss produced during Peak1 corresponds to the overlapping of the gases released during stages 1 (H_2O) and 2 ($C_xH_xO_x$ and C_xH_x) of the pyrolysis of the phenolic resin, whereas Peak2 corresponds to stages 3 (CO, CH_4, C_xH_x) and 4 (H_2).

In this case, there is also a systematic variation on the final char (~1%) by using a lid during the experiments, providing a $p^{95\%}_{\text{value}} = 1.3 \times 10^{-3}$ in a confidence level of 95%. As for niaouli, one observes that the use of a lid increases the char production (Fig. 7b).

B. Identification of Kinetic Parameters with FiTGA

In the previous section, we showed that differences in experimental conditions can affect the final char yield, presumably due to secondary reactions. Because we are only interested on the pyrolysis phenomenon itself, the extraction of the kinetic parameters has been carried out with the data obtained when not using a lid, thus having a rapid evacuation of the gases and avoiding secondary char formation reactions.

1. *Niaouli*

It is known that the use of parallel schemes in biomass does not allow to reproduce large varying conditions [24]. However, because the range of heating rates considered in this study is relatively small ($\beta = 5$–40 K $\cdot$ min^{-1}), it was considered interesting to extract kinetic parameters for the data obtained using FiTGA.

Three reactions were considered for the decomposition of niaouli based on its three main components (cellulose, hemicellulose, and lignin) [23] as seen in the kinetic scheme depicted in Fig. 8. Thus, carrying out the parameter identification after evaporation of water (first experimentally observed peak) had finished.

Figure 9 shows a comparison between the experimental TGA curves and the calculated ones using FiTGA. It can be observed that FiTGA is capable of reproducing with good accuracy the mass loss evolution (TGA, top) as well as its derivative (DTGA, bottom). The shadowed areas on the DTGA graphs correspond to the different contributions from each reaction (Fig. 8). One can distinguish the fast pyrolysis of hemicellulose and cellulose with narrow peaks, and the slower pyrolysis of lignin with a much wider and extended peak. It can be seen that even though three peaks are recovered by FiTGA, they do not perfectly match the experimental observations. They overlap because pyrolysis of all three wood components occurs simultaneously in a narrow temperature range. This hinders the parameter identification through optimization. In addition, one can observe a slight difference on the final mass loss of niaouli at $\beta = 40$ K $\cdot$ min^{-1}. Changes on char yield cannot be captured by multicomponent schemes because the constants F_i specify how much mass is lost by each reaction. The kinetic parameters recovered are provided in Table 2. Despite the observed differences, the activation energy ($\mathcal{E}_i$), the parameter that triggers the reactions, recovered by FiTGA for niaouli remains on the same order of magnitude as for other biomass species [24].

2. *ZURAM*

For ZURAM, we decided to use a scheme with four global reactions based on results from different researchers [20,30,51,52],

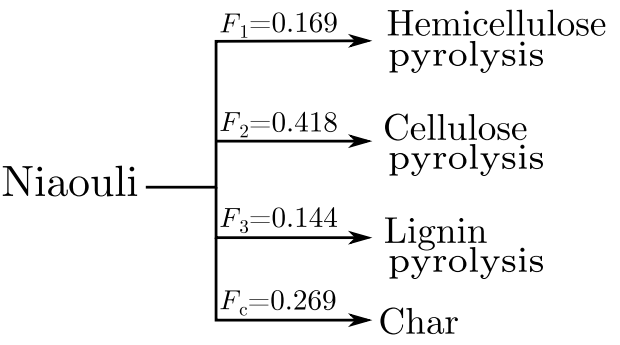

Fig. 8 Parallel scheme proposed for decomposition of niaouli.

[§§]The smaller y-axis scale makes the DGTA signal in Fig. 6b appear more noisy than in Fig. 6a.

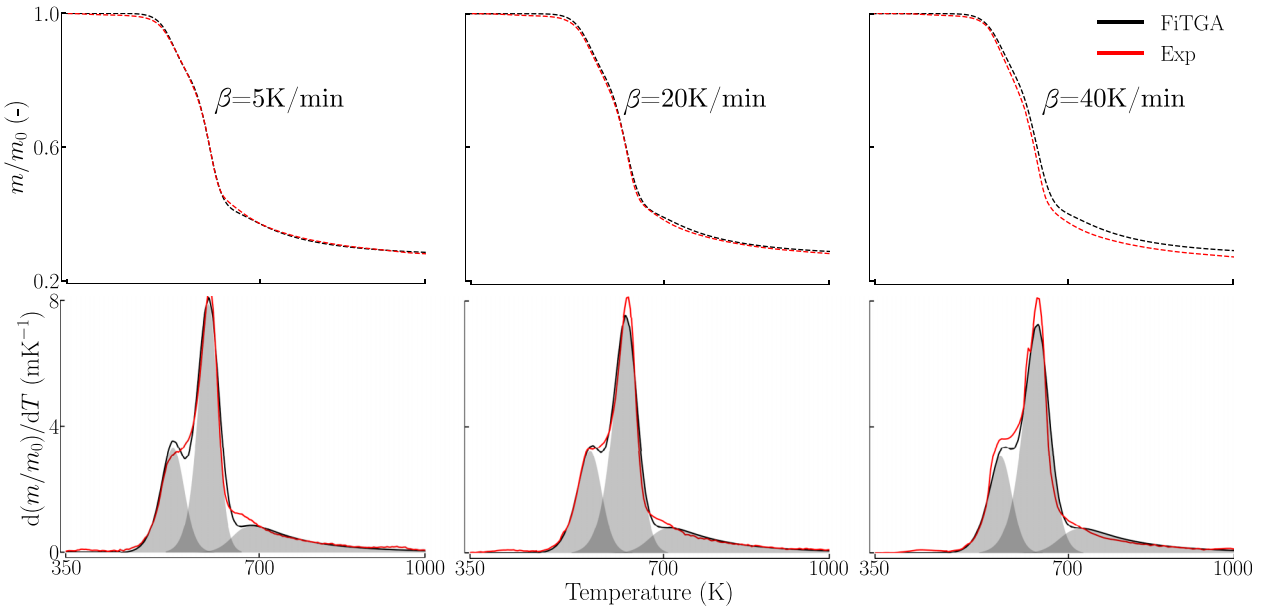

Fig. 9 Comparison between experiments and parameters recovered by FiTGA for niaouli. The model can reproduce the mass loss; however, the shoulders are not accurately captured in the DTGA. Shadowed areas represent contribution of each reaction.

Table 2 Arrhenius parameters for three parallel reaction mechanism of niaouli

Parameters	Hemicellulose	Cellulose	Lignin
F	0.169	0.418	0.144
n	1.45	1.45	7.27
$\log(\mathcal{A})$	11.69	13.49	14.22
$\mathcal{E}$, kJ · mol^{-1}	145.5	184.0	219.9

where four main stages of pyrolysis were identified on similar materials by using gas chromatography (GC) and mass spectrometry (MS) to measure the generated gases. Figure 10 depicts the four reactions as well as the mass fractions F_i corresponding to each reaction.

Our fitted curves, presented in Fig. 11, show that FiTGA recovers a set of parameters that are capable of reproducing the mass loss of ZURAM for the studied heating rates. The shape of the DTGA is also well captured with its two main decomposition peaks. The slight

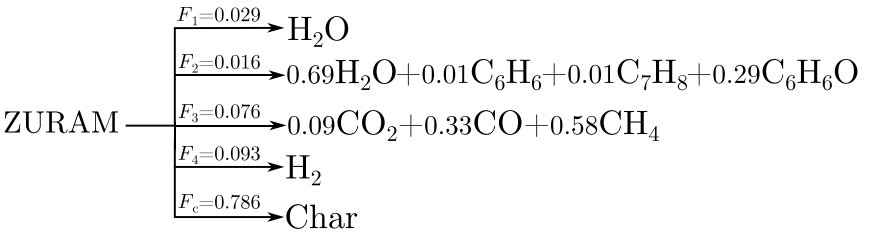

Fig. 10 Parallel scheme proposed for decomposition of ZURAM based on TACOT model.

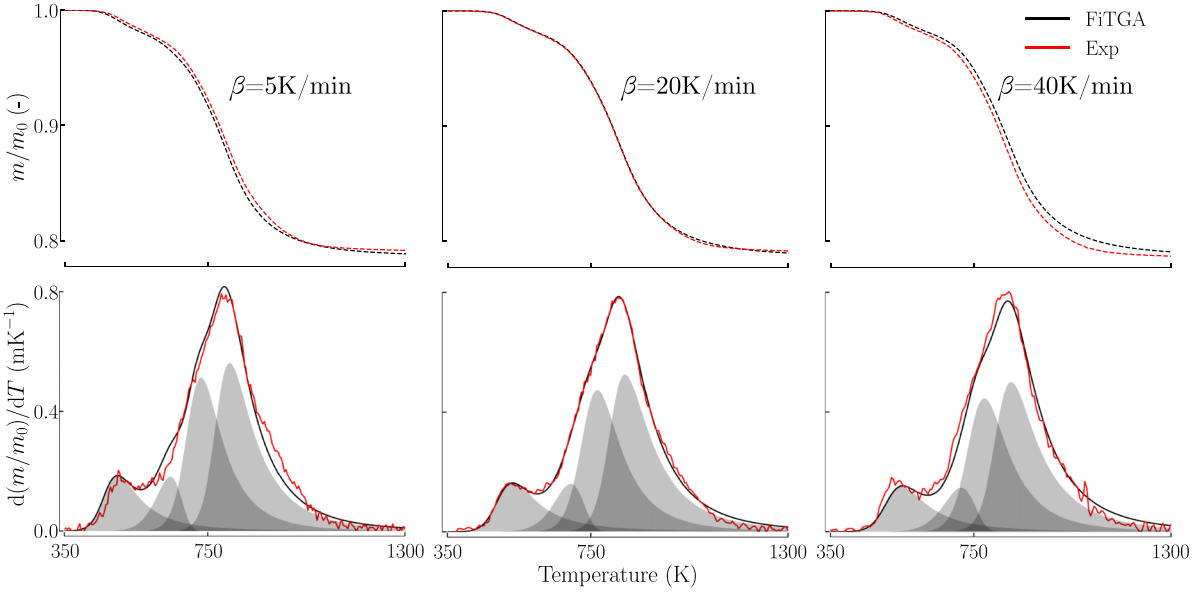

Fig. 11 Comparison between experiments and parameters recovered by FiTGA for ZURAM. The model is capable of capturing the thermal degradation of ZURAM with great accuracy. Shadowed areas represent contribution of each reaction.

Table 3 Arrhenius parameters for four parallel reaction mechanism of

Parameters	R1	R2	R3	R4
F	0.029	0.016	0.076	0.093
n	4.41	1.00	3.59	4.59
$\log(\mathcal{A})$	5.98	4.96	9.11	11.56
$\mathcal{E}$, kJ · mol^{-1}	81.6	93.5	163.2	218.6

difference on the mass loss observed for the heating rate of $\beta = 40$ K · min^{-1} may be attributed to a change on the degradation process toward higher heating rates. This effect, however, cannot be studied with the current setup due to limitations on the TGA device. Further investigations are required for the extrapolation of this kinetic scheme toward higher heating rates.

Table 3 presents a summary of the obtained kinetic parameters of ZURAM. These results are on the same order of magnitude as the ones reported by Lachaud et al. [29]. This indicates that the thermal degradation of ZURAM via pyrolysis is somehow similar to that of the phenolic impregnated carbon ablator of NASA.

V. Conclusions

In this work, the same methodology has been applied to study two types of materials: TPS and biomass. These two materials share similarities in the microstructure and the thermal degradation via pyrolysis.

Niaouli presents a similar behavior to other biomass species with four decomposition peaks on the DTGA curve, suggesting the evaporation of water and the pyrolysis of hemicellulose, cellulose, and lignin, respectively with increasing temperature. Pyrolysis gets complete at $T \approx 800$ K with a mass loss of ∼75%. Using a pierced lid to cover the crucibles during pyrolysis promotes char production with an increase of 3% when compared with the case of open crucible.

In turn, the decomposition of ZURAM presents two main peaks located at $T_{\text{peak1}} \approx 500$ K and $T_{\text{peak2}} \approx 800$ K, with a mass loss of ∼20% at completion of pyrolysis ($T \approx 1100$ K). As for biomass, using a lid has promoted char generation, in this case by 1%.

Even though an analogy between TPS and biomass has been presented, the pyrolysis process occurs differently for the two materials. Niaouli undergoes a greater mass loss than ZURAM. This is mainly because cellulose, fiber component for biomass, will also pyrolyze, whereas the carbon fibers will not. In addition, the pyrolysis of ZURAM occurs across a wide range of temperatures (400–1000 K); for niaouli it occurs in a narrower range (550–800 K).

The degradation of a lightweight carbon/phenolic ablator for TPS (ZURAM) has been characterized, providing reference data for material response code validation.

Multicomponent kinetic mechanisms have been proposed for the pyrolysis of ZURAM and niaouli at low heating rates. In both cases, the mass loss evolution is accurately described by the proposed models.

However, this does not ensure extrapolation toward high heating rates, which should be carefully assessed using other type of experiments such as cone calorimetry or drop tube. In addition, other experimental techniques, such as differential scanning calorimetry or GC, would provide a greater understanding on the decomposition process.

An accurate pyrolysis kinetic scheme validated over a large range of heating conditions would improve the current predictions by having more accurate estimates on the mass loss rate as well as on the energy consumed during the decomposition, which are essential for an optimal TPS design.

Appendix: Summary of Experiments

In the following, test matrix tables are included for both niaouli and ZURAM. These tables include essential information such as the heating rate used, the initial and final mass, and if the measurement was performed using a lid.

Table A1 Experimental measurements of niaouli

Case	β, $K \cdot$ min^{-1}	Lid?	Initial mass, mg	Mass loss, %	Final mass, mg
Niaouli 5 #1	5	No	32.58	76.73	7.58
Niaouli 5 #2	5	No	28.07	77.52	6.31
NiaouliLid 5 #1	5	Yes	28.69	73.33	7.65
NiaouliLid 5 #2	5	Yes	27.04	73.73	7.10
Niaouli 20 #1	20	No	26.88	76.57	6.30
Niaouli 20 #2	20	No	24.71	77.88	5.47
Niaouli 20 #3	20	No	25.89	77.30	5.88
Niaouli 20 #4	20	No	31.66	76.81	7.34
NiaouliLid 20 #1	20	Yes	27.31	73.23	7.31
NiaouliLid 20 #2	20	Yes	29.83	73.75	7.83
Niaouli 40 #1	40	No	33.25	76.64	7.77
Niaouli 40 #2	40	No	28.74	77.11	6.58
NiaouliLid 40 #1	40	Yes	33.17	74.38	8.50
NiaouliLid 40 #2	40	Yes	25.91	74.82	6.53

Table A2 Experimental measurements of ZURAM®

Case	β, K · min^{-1}	Lid?	Initial mass, mg	Mass loss, %	Final mass, mg
ZURAM® 5 #1	5	No	28.94	22.68	22.38
ZURAM® 5 #2	5	No	24.40	23.36	18.70
ZURAM®Lid 5 #1	5	Yes	23.61	21.10	18.62
ZURAM®Lid 5 #2	5	Yes	29.14	21.51	22.88
ZURAM® 10 #1	10	No	23.85	21.64	18.69
ZURAM® 10 #2	10	No	26.18	22.07	20.40
ZURAM® 20 #1	20	No	29.32	22.28	22.79
ZURAM® 20 #2	20	No	27.99	22.46	21.70
ZURAM® 20 #3	20	No	32.83	21.80	25.67
ZURAM®Lid 20 #1	20	Yes	26.28	20.87	20.80
ZURAM®Lid 20 #2	20	Yes	29.44	21.31	23.16
ZURAM® 40 #1	40	No	29.64	21.94	23.13
ZURAM® 40 #2	40	No	26.91	22.28	20.92
ZURAM®Lid 40 #1	40	Yes	27.64	21.55	21.69
ZURAM®Lid 40 #2	40	Yes	23.87	21.55	18.73

Acknowledgments

The research of F. T.-H., V. L., and T. E. M. is sponsored by the European Research Council Proof of Concept Grant # 713726. The samples of the ablator studied in this project were provided through the European Space Agency (ESA) Research Program ABLARADABLA project # ESA ITT AO/1-7987/14/NL/RA. Niaouli samples were provided through the European Research Council Proof of Concept Grant # 713726. We would like to thank Gregory Pinaud (ArianeGroup) for his suggestions on the fitting algorithm. Gertjan Glabeke von Karman Institute (VKI) is acknowledged for his support during the experimental campaign. Christian Zuber and Thomas Reimer (German Aerospace Center [DLR] Stuttgart) are acknowledged for providing characterization support and information regarding the production of ZURAM®.

References

[1] Tran, H. K., "Development of Lightweight Ceramic Ablators and Arc-Jet Test Results," NASA TM-108798, Jan. 1994, https://ntrs.nasa.gov/search.jsp?R=19940028611.

[2] Tran, H., Johnson, C., Rasky, D., Hui, F., Hsu, M. T., Chen, T., Chen, Y. K., Paragas, D., and Kobayashi, L., "Phenolic Impregnated Carbon Ablators (PICA) as Thermal Protection Systems for Discovery Missions," NASA TM-110440, April 1997, https://ntrs.nasa.gov/search.jsp?R=19970017002.

[3] Stackpoole, M., Sepka, S., Cozmuta, I., and Kontinos, D., "Post-Flight Evaluation of Stardust Sample Return Capsule Forebody Heatshield Material," *46th AIAA Aerospace Sciences Meeting and Exhibit*, AIAA Paper 2008-1202, 2008. https://doi.org/10.2514/6.2008-1202

[4] Edquist, K. T., Hollis, B. R., Johnston, C. O., Bose, D., White, T. R., and Mahzari, M., "Mars Science Laboratory Heat Shield Aerothermodynamics: Design and Reconstruction," *Journal of Spacecraft and Rockets*, Vol. 51, No. 4, 2014, pp. 1106–1124. https://doi.org/10.2514/1.A32749

[5] Turchi, A., Bianchi, D., Nasuti, F., and Onofri, M., "A Numerical Approach for the Study of the Gas–Surface Interaction in Carbon–Phenolic Solid Rocket Nozzles," *Aerospace Science and Technology*, Vol. 27, No. 1, 2013, pp. 25–31, http://www.sciencedirect.com/science/article/pii/S1270963812001010.

[6] Wright, M. J., Bose, D., and Chen, Y.-K., "Probabilistic Modeling of Aerothermal and Thermal Protection Material Response Uncertainties," *AIAA Journal*, Vol. 45, No. 2, 2007, pp. 399–410. https://doi.org/10.2514/1.26018

[7] Zhong, J., Ozawa, T., and Levin, D. A., "Modeling of Stardust Reentry Ablation Flows in the Near-Continuum Flight Regime," *AIAA Journal*, Vol. 46, No. 10, 2008, pp. 2568–2581. https://doi.org/10.2514/1.36196

[8] Laub, B., and Venkatapathy, E., "Thermal Protection System Technology and Facility Needs for Demanding Future Planetary Missions," *International Workshop Planetary Probe Atmospheric Entry and Descent Trajectory Analysis and Science*, Vol. 544, ESA Publications Division, Lisbon, 2004, pp. 239–247, http://adsabs.harvard.edu/abs/2004ESASP.544.239L.

[9] Duffa, G., *Ablative Thermal Protection Systems Modeling*, AIAA, Reston, VA, 2013, Chap. 1.

[10] Wright, M., Cozmuta, I., Laub, B., Chen, Y.-K., and Wilcoxson, W. H., "Defining Ablative Thermal Protection System Margins for Planetary Entry Vehicles," *42nd AIAA Thermophysics Conference*, AIAA Paper 2011-3757, 2011.

[11] Di Blasi, C., "Modeling Chemical and Physical Processes of Wood and Biomass Pyrolysis," *Progress in Energy and Combustion Science*, Vol. 34, No. 1, 2008, pp. 47–90, http://www.sciencedirect.com/science/article/pii/S0360128507000214.

[12] Couhert, C., Commandre, J.-M., and Salvador, S., "Is It Possible to Predict Gas Yields of Any Biomass After Rapid Pyrolysis at High Temperature from Its Composition in Cellulose, Hemicellulose and Lignin?" *Fuel*, Vol. 88, No. 3, 2009, pp. 408–417. https://doi.org/10.1016/j.fuel.2008.09.019

[13] Broido, A., and Kilzer, F. J., "A Critique of the Present State of Knowledge of the Mechanism of Cellulose Pyrolysis," *Fire Research Abstracts and Reviews*, Vol. 5, No. 2, 1963, pp. 157–161, https://www.fs.usda.gov/treesearch/pubs/50133.

[14] Goldstein, H. E., "Pyrolysis Kinetics of Nylon 6–6, Phenolic Resin, and Their Composites," *Journal of Macromolecular Science: Part A—Chemistry*, Vol. 3, No. 4, 1969, pp. 649–673. https://doi.org/10.1080/10601326908053834

[15] Lachaud, J., "A Pragmatic Model for High-Temperature Porous Reactive Materials, with Application to Ablation and Biomass Pyrolysis," *STO-AVT-261 Porous Media Interaction with High Temperature and High Speed Flows*, von Karman Institute, Rhode-Saint-Genese, Belgium, 2015, Chap. 9.

[16] Torres-Herrador, F., Meurisse, J. B. E., Panerai, F., Blondeau, J., Lachaud, J., Bessire, B. K., Magin, T. E., and Mansour, N. N., "A High Heating Rate Pyrolysis Model for the Phenolic Impregnated Carbon Ablator (PICA) Based on Mass Spectroscopy Experiments," *Journal of Analytical and Applied Pyrolysis*, Vol. 100, Aug. 2019, Paper 104625, http://www.sciencedirect.com/science/article/pii/S0165237019301603.

[17] Torres-Herrador, F., Coheur, J., Panerai, F., Magin, T. E., Arnst, M., Mansour, N. N., and Blondeau, J., "Competitive Kinetic Model for the Pyrolysis of the Phenolic Impregnated Carbon Ablator," *Aerospace Science and Technology*, Vol. 100, May 2020, Paper 105784, http://www.sciencedirect.com/science/article/pii/S1270963819332031.

[18] Toraman, H. E., Vanholme, R., Borén, E., Vanwonterghem, Y., Djokic, M. R., Yildiz, G., Ronsse, F., Prins, W., Boerjan, W., Van Geem, K. M., and Marin, G. B., "Potential of Genetically Engineered Hybrid Poplar for Pyrolytic Production of Bio-Based Phenolic Compounds," *Bioresource Technology*, Vol. 207, May 2016, pp. 229–236. https://doi.org/10.1016/j.biortech.2016.02.022.

[19] Wong, H.-W., Peck, J., Assif, J., Panerai, F., Lachaud, J., and Mansour, N. N., "Detailed Analysis of Species Production from the Pyrolysis of the Phenolic Impregnated Carbon Ablator," *Journal of Analytical and Applied Pyrolysis*, Vol. 122, Nov. 2016, pp. 258–267, http://www.sciencedirect.com/science/article/pii/S016523701630211X.

[20] Bessire, B. K., and Minton, T. K., "Decomposition of Phenolic Impregnated Carbon Ablator (PICA) as a Function of Temperature and Heating Rate," *ACS Applied Materials & Interfaces*, Vol. 9, No. 25, 2017, pp. 21,422–21,437. https://doi.org/10.1021/acsami.7b03919

[21] Ceglia, G., Trifoni, E., Gouriet, J.-B., Chazot, O., Mareschi, V., Rufolo, G., and Tumino, G., "Experimental Investigation on IXV TPS Interface Effects in Plasmatron," *CEAS Space Journal*, Vol. 8, No. 2, 2016, pp. 65–75. https://doi.org/10.1007/s12567-015-0108-y

[22] Marocco, R., Schiariti, D., Paglia, F., Signorelli, M., Pippia, G., Di Vita, G., Rufolo, G., Chazot, O., and Helber, B., "Ablative Thermal Protection for IXV: Experimental Data and Numerical Simulations," *European Space Agency (Special Publication) ESA SP*, Vol. 705, 2013.

[23] Shafizadeh, F., and Chin, P., "Thermal Deterioration of Wood," *Wood Technology: Chemical Aspects*, ACS Symposium Series, Vol. 43, American Chemical Soc., Washington, 1977, pp. 57–81, https://doi.org/10/cx27mm.

[24] Park, W. C., Atreya, A., and Baum, H. R., "Experimental and Theoretical Investigation of Heat and Mass Transfer Processes During Wood Pyrolysis," *Combustion and Flame*, Vol. 157, No. 3, 2010, pp. 481–494. https://doi.org/10/1016/j.combustflame.2009.10.006

[25] Domingo, F. V., Rodrigo, L. C., and Greus, A. R., *Thermal Characterisation of Polymeric Materials*, Univ. Politècnica de València, Valencia, Spain, 2008, Chap. 2.

[26] Agarwal, R. K., "On the Use of the Arrhenius Equation to Describe Cellulose and Wood Pyrolysis," *Thermochimica Acta*, Vol. 91, Sept. 1985, pp. 343–349, http://www.sciencedirect.com/science/article/pii/0040603185852278.

[27] Vyazovkin, S., "Kinetic Concepts of Thermally Stimulated Reactions in Solids: A View from a Historical Perspective," *International Reviews in Physical Chemistry*, Vol. 19, No. 1, 2000, pp. 45–60. https://doi.org/10.1080/014423500229855

[28] Simon, P., "Single-Step Kinetics Approximation Employing Non-Arrhenius Temperature Functions," *Journal of Thermal Analysis and Calorimetry*, Vol. 79, No. 3, 2005, pp. 703–708, https://link.springer.com/article/10.1007/s10973-005-0599-4.

[29] Lachaud, J., Scoggins, J. B., Magin, T. E., Meyer, M. G., and Mansour, N. N., "A Generic Local Thermal Equilibrium Model for Porous Reactive Materials Submitted to High Temperatures," *International Journal of Heat and Mass Transfer*, Vol. 108, May 2017, pp. 1406–1417. https://doi.org/10.1016/j.ijheatmasstransfer.2016.11.067

[30] Trick, K. A., Saliba, T. E., and Sandhu, S. S., "A Kinetic Model of the Pyrolysis of Phenolic Resin in a Carbon/Phenolic Composite," *Carbon*, Vol. 35, No. 3, 1997, pp. 393–401. https://doi.org/10.1016/S0008-6223(97)89610-8

[31] Rothermel, T., Herdrich, G., Walpot, L., and Zuber, C., "A Light-Weight Ablative Material for Research Purposes," *6th Ablation Workshop*, Univ. of Kentucky, 2014.

[32] van Eekelen, T., Cozmuta, I., Martin, A., and Lachaud, J., "Ablation Test Case 3," *6th Ablation Workshop*, 2014.

[33] Helber, B., Asma, C. O., Babou, Y., Hubin, A., Chazot, O., and Magin, T. E., "Material Response Characterization of a Low-Density Carbon Composite Ablator in High-Enthalpy Plasma Flows," *Journal of Materials Science*, Vol. 49, No. 13, 2014, pp. 4530–4543. https://doi.org/10.1007/s10853-014-8153-z

[34] Helber, B., Chazot, O., Magin, T., and Hubin, A., "Ablation of Carbon Preform in the VKI Plasmatron," *43rd AIAA Thermophysics Conference*, AIAA Paper 2012-2876, 2012. https://doi.org/10.2514/6.2012-2876

[35] Helber, B., Turchi, A., Scoggins, J. B., Hubin, A., and Magin, T. E., "Experimental Investigation of Ablation and Pyrolysis Processes of Carbon-Phenolic Ablators in Atmospheric Entry Plasmas," *International Journal of Heat and Mass Transfer*, Vol. 100, Sept. 2016, pp. 810–824. https://doi.org/10.1016/j.ijheatmasstransfer.2016.04.072

[36] Meurisse, J. B. E., Lachaud, J., Panerai, F., Tang, C., and Mansour, N. N., "Multidimensional Material Response Simulations of a Full-Scale Tiled Ablative Heatshield," *Aerospace Science and Technology*, Vol. 76, May 2018, pp. 497–511, http://www.sciencedirect.com/science/article/pii/S1270963817323179.

[37] Bryden, K. M., Ragland, K. W., and Rutland, C. J., "Modeling Thermally Thick Pyrolysis of Wood," *Biomass and Bioenergy*, Vol. 22, No. 1, 2002, pp. 41–53. https://doi.org/10.1016/S0961-9534(01)00060-5

[38] Di Blasi, C., and Branca, C., "Kinetics of Primary Product Formation from Wood Pyrolysis," *Industrial & Engineering Chemistry Research*, Vol. 40, No. 23, 2001, pp. 5547–5556. https://doi.org/10.1021/ie000997e

[39] Murienne, J., "New Caledonia, Biology," *Encyclopedia of Islands*, 2009, pp. 643–645.

[40] "Interpreting DSC Curves," *Thermal Analysis UserCom*, Mettler-Toledo, 2000, http://us.mt.com/content/us/en/home/supportive_content/usercom/TA_UserCom11.html.

[41] Blondeau, J., "Investigation of Pulverised Biomass Combustion: Detailed Modelling of Particle Pyrolysis and Experimental Analysis of Ash Deposition," Ph.D. Thesis, Univ. catholique de Louvain, Ottignies-Louvain-la-Neuve, Belgium, May 2013.

[42] Brown, M. E., Maciejewski, M., Vyazovkin, S., Nomen, R., Sempere, J., Burnham, A., Opfermann, J., Strey, R., Anderson, H. L., Kemmler, A., et al., "Computational Aspects of Kinetic Analysis: Part A: The ICTAC Kinetics Project-Data, Methods and Results," *Thermochimica Acta*, Vol. 355, Nos. 1–2, 2000, pp. 125–143. https://doi.org/10.1016/S0040-6031(00)00443-3

[43] Rath, J., Wolfinger, M. G., Steiner, G., Krammer, G., Barontini, F., and Cozzani, V., "Heat of Wood Pyrolysis," *Fuel*, Vol. 82, No. 1, 2003, pp. 81–91. https://doi.org/10.1016/S0016-2361(02)00138-2

[44] "Investigating Unknown Samples," *Thermal Analysis UserCom*, Mettler-Toledo, 1997, http://us.mt.com/content/us/en/home/supportive_content/usercom/TA_UserCom29.html.

[45] Coleman, T., and Li, Y., "An Interior Trust Region Approach for Nonlinear Minimization Subject to Bounds," *SIAM Journal on Optimization*, Vol. 6, No. 2, 1996, pp. 418–445. https://doi.org/10.1137/0806023

[46] Duan, Q. Y., Gupta, V. K., and Sorooshian, S., "Shuffled Complex Evolution Approach for Effective and Efficient Global Minimization," *Journal of Optimization Theory and Applications*, Vol. 76, No. 3, 1993, pp. 501–521. https://doi.org/10.1007/BF00939380

[47] Goldberg, D. E., *Genetic Algorithms in Search, Optimization, and Machine Learning*, Addison-Wesley, Boston, 1989, Chap. 3.

[48] Roberts, A. F., "The Heat of Reaction During the Pyrolysis of Wood," *Combustion and Flame*, Vol. 17, No. 1, 1971, pp. 79–86, http://www.sciencedirect.com/science/article/pii/S0010218071801414.

[49] Mok, W. S. L., and Antal, M. J., "Effects of Pressure on Biomass Pyrolysis. II. Heats of Reaction of Cellulose Pyrolysis," *Thermochimica Acta*, Vol. 68, No. 2, 1983, pp. 165–186. https://doi.org/10.1016/0040-6031(83)80222-6

[50] Wong, H.-W., Peck, J., Bonomi, R. E., Assif, J., Panerai, F., Reinisch, G., Lachaud, J., and Mansour, N. N., "Quantitative Determination of Species Production from Phenol-Formaldehyde Resin Pyrolysis," *Polymer Degradation and Stability*, Vol. 112, Feb. 2015, pp. 122–131. https://doi.org/10.1016/j.polymdegradstab.2014.12.020

[51] Wong, H.-W., Peck, J., Edwards, R., Reinisch, G., Lachaud, J., and Mansour, N. N., "Measurement of Pyrolysis Products from Phenolic Polymer Thermal Decomposition," *52nd Aerospace Sciences Meeting*, AIAA Paper 2014-1388, 2015. https://doi.org/10.2514/6.2014-1388

[52] Bessire, B. K., Lahankar, S. A., and Minton, T. K., "Pyrolysis of Phenolic Impregnated Carbon Ablator (PICA)," *ACS Applied Materials & Interfaces*, Vol. 7, No. 3, 2015, pp. 1383–1395. https://doi.org/10.1021/am507816f

J. Poggie
Associate Editor